Desalination and Water Treatment
www.deswater.com

doi: 10.5004/dwt.2017.21051

84 (2017) 59–68
July

Removal of hardness from RO concentrate of paper mill effluents with NF membrane for water reuse

Wei Yan, Weixing Li, Fei Liu, Ming Zhou, Weihong Xing*

State Key Laboratory of Materials-Oriented Chemical Engineering, National Engineering Research Center for Special Separation Membrane, Nanjing Tech University, Nanjing 210009, China, Tel. +86-25-8317-2288; Fax: +86-25-8317-2292; emails: xingwh@njtech.edu.cn (W. Xing), yanttxs@163.com (W. Yan), wxli@njtech.edu.cn (W. Li), 642081701069@njtech.edu.cn (F. Liu), mingzhou@njtech.edu.cn (M. Zhou)

Received 22 January 2017; Accepted 17 June 2017

ABSTRACT

Nanofiltration (NF) membrane was used to eliminate hardness (Ca^{2+} and Mg^{2+}) from reverse osmosis (RO) concentrate of paper mill effluents in order to realize the on-site water reuse. It has been found that cross-flow velocity had significant effect on the membrane separation efficiency. Total hardness in the RO concentrate was reduced from 1,047 to 433 mg/L and the removal ratio of hardness was as high as 84% in the concentration mode of filtration experimented in the lab. The NF permeate was collected as recovered water fulfilling the reuse standard on hardness, sulfates, chemical oxygen demands, total dissolved solid, etc. In another 114 h test carried out at the factory, the water flux of the membrane was kept constant as 15 L/m^2/h and the rejection of hardness maintained as 76%. Volumetric charge density (X_d) of the membrane was intensified with increasing concentration of $CaCl_2$ from 1 to 10 mol/m^3 in solution. It helps to clarify the enhanced desalination efficiency (in particular the scaling ions) by the membrane at higher concentration of feed. In a conclusion, NF membrane process has been investigated and proven as an effective water treatment approach following RO process to improve industrial water recovery without utilizing additional chemicals.

Keywords: NF membrane process; Paper mill effluents; RO concentrate; Water reuse

1. Introduction

Pulp and paper industry has considerable consumption of freshwater and produces large amount of wastewater. It is urgent to reduce freshwater consumption and minimize wastewater treatment plant [1,2]. Typical methods to eliminate a variety of contaminants from the produced wastewater have been intensively studied over the past two decades including sedimentation, floatation, coagulation, precipitation, adsorption, advanced oxidation and membrane processes [3,4].

Membrane technologies, reverse osmosis (RO) in particular, have attracted increasing attention as an advanced treatment to paper mill effluents. The RO concentrate from such effluents is often high in salinity, hardness and chemical oxygen demand (COD) and has severe impact on ecosystems and human health [5]. However, the discharge management of RO concentrate still remains problematical due to insufficient alternatives [6]. Conventional treatment techniques include coagulation, activated carbon adsorption, ozonation and Fenton process. More recent development involves processes such as photocatalysis, photooxidation, sonolysis and electrochemical oxidation [7–9]. These treating methods have good efficiency in removing CODs, yet lack the feasibility to eliminate scaling ions from the wastewater.

Nanofiltration (NF) membrane process, governed primarily by steric hindrance and Donnan exclusion mechanisms, is a pressure-driven separation process with mean membrane pore size between RO and ultrafiltration (UF) [10]. NF process is an innovative technique to purify RO concentrate having advantages of high rejection to both polyvalent ions and CODs (no additional chemical needed) and the high flux

* Corresponding author.

under relatively low pressure (i.e., lower energy consumption) [6,11–16]. Many studies have pointed out that operating parameters in NF process affect the efficiency of hardness removal and water recovery [16–20]. The study by Gonzalez et al. [6] proved that NF270 membrane was very useful in separating polyvalent and monovalent anions from RO desalination brines and the rejection to Cl^- could be as low as –2%, making this membrane suitable to enhance water recovery of RO concentrate. Tonko et al. [16] investigated the opportunities of preventing ions scaling from thermal water by DK membrane which has achieved high removal of total hardness with stable water flux. As for optimizing a membrane process, Taguchi design is the widely used method to optimize the process within orthogonal array, requiring less times of exploring tests [21–23]. In parallel, analysis of variance (ANOVA) is a statistical means to evaluate the importance of each experimental parameter in the process [24–26].

Objective of the work is to improve the water recovery and the water quality in paper industry wastewater by employing the NF membrane process in the treatment workstream. Membrane rejection to the scaling ions is enhanced by adjusting operative parameters including cross-flow velocity (CFV), transmembrane pressure (TMP) and volume reduction factor (VRF) in the NF process. Working conditions leading to the highest efficiency of hardness removal were found in the experiments designed in Taguchi array. Significance of each parameter was analyzed in ANOVA statistical calculation. Long-term performance of DL membrane was examined more than 100 h on the site of paper mill factory. Concentration effect on membrane separation behavior was additionally studied using model solution $CaCl_2/H_2O$.

2. Experimental setup

2.1. Feed, membrane and membrane unit

RO concentrate of paper mill effluents was obtained from a dual membrane UF/RO process facilitated in Gold Hongye Paper Group, Suzhou, China. Such concentrated wastewater was used as feed solution in the Taguchi-designed experiments and the long-term test of NF membrane process.

DL NF membrane manufactured by General Electric Company (GE) was used in this study. It is a polyamide composite membrane in spiral wound module, which has 96% rejection in $MgSO_4$ solution (2 g/L) at TMP 0.69 MPa according to the manufacturer report. The effective filtration area of membrane (A) is 0.325 m^2 and the molecular weight cut-off is 150–300 Da. The membrane is bearable to pH from 2 to 11, temperature up to 50°C and TMP 4.14 MPa. Scanning electron microscopic (SEM) surface and cross-section images of DL are displayed in Fig. 1. Scanned membrane surface is smooth and defect-free. Upmost separation layer (polyamide) and macroporous support layer (polysulfone) can be well observed in the cross-section images (with zoomed one on the right). Thickness of polyamide separation layer is estimated around 200 nm according to SEM. Pores in the membrane are with tortuosity structure.

Membrane unit, equipped with a spiral-wound module, was in cross-flow setup as illustrated in Fig. 2. The wastewater was pumped from the feed tank to the membrane with a plunger pump. TMP and CFV in the flow were modulated through valve 5 and value 6. Experiments following the Taguchi design were conducted in concentration mode of filtration: permeate solution (V_p) was collected in a container separately and the retentate solution (V_r) was immediately circulated back to the feed solution (V_f). The temperature of feed solution was kept constantly at 30°C by cooling water. Testing continued until the VRF value was reached to a certain level, which is calculated using the following equation:

$$\mathrm{VRF} = \frac{V_f}{V_r} \tag{1}$$

where V_f is the initial volume of feed and V_r is the volume of retentate.

After each Taguchi experiment, the membrane module was cleaned with deionized water (conductivity < 20 μS/cm) for three times. And the pure water flux through membrane was regained above 98% of the initial level.

Further on, in a long-term membrane test the feed solution was continuously supplied with fresh RO concentrate and both permeate and retentate solutions were discharged away. On the other hand, in the experiments of concentration study (using $CaCl_2/H_2O$ as model solution) permeate and retentate solutions were always circulated back to the feed tank.

2.2. Characterization on the membrane performance

The pH value of RO concentrate from paper mill factory was measured with a ZDJ-4A pH meter (INESA, China). The conductivity and total dissolved solid (TDS) measurement were carried out by using DDSJ-308A (INESA, China). The concentrations of metal cations were quantified with inductively coupled plasma atomic emission spectrometer (ICP-AES; PerkinElmer, USA), and the concentrations of anions were determined by ion chromatograph (ICS 2000, DIONEX, USA). COD was examined by DR1010 tester (HACH, USA). Turbidity was measured using 2100N turbidimeter (HACH, USA) and silt density index (SDI) was examined with home-made SDI Analyzer. Zeta-potential (ζ) was measured with SurPASS Electrokinetic Analyzer (Anton Paar, Austria). All samples were examined not less than three times and relative errors were smaller than 5%. Microstructure of DL membrane was observed with SEM (S-4800, Hitachi, Japan). The samples for cross-section scanning were prepared in liquid nitrogen.

CFV value is calculated with Eq. (2):

$$\mathrm{CFV} = \frac{Q}{A_o} \tag{2}$$

where Q is flow rate, and cross-sectional area of membrane A_o was 7.34×10^{-4} m^2 according to the length of unfolded spiral wound membrane (0.85 m) and the spacer thickness (8.63×10^{-4} m).

The water flux (J) is expressed as follows:

$$J = \frac{1}{A}\frac{\Delta V}{\Delta t} \tag{3}$$

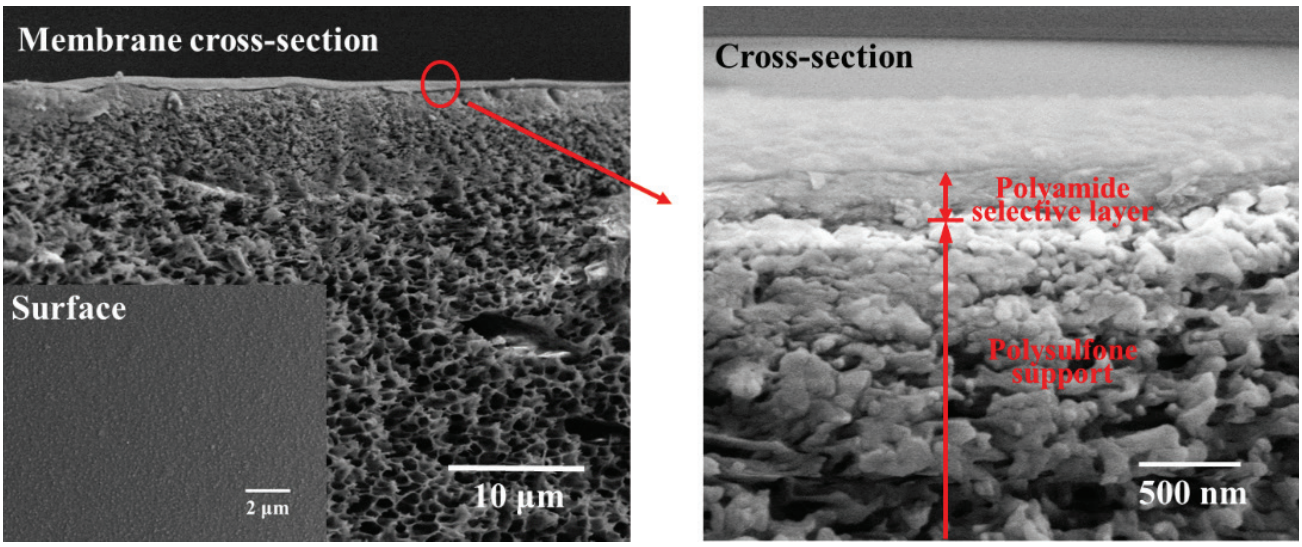

Fig. 1. SEM surface and cross-section images of the NF membrane.

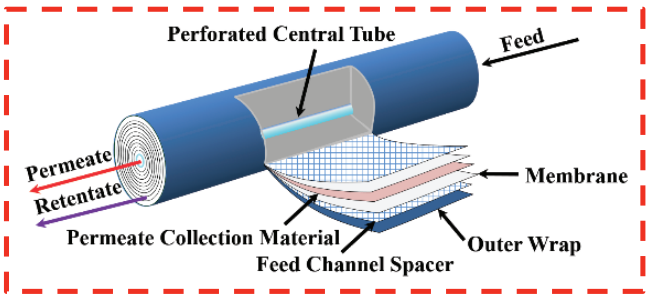

Fig. 2. The setup of the membrane unit: (1) experiments using RO concentrate as the feed (valves 3 and 4 closed), (2) the 114 h long-term experiment (valves 1 and 4 closed) and (3) experiments using model solution as the feed (valves 2 and 3 closed).

where A is the effective filtration area of membrane (0.325 m^2), ΔV is the permeate volume and Δt is the permeate time.

Total hardness of Ca^{2+} and Mg^{2+} in water is given by Eq. (4) using $CaCO_3$ as the calibration standard (molecule weight = 100):

$$\text{Total hardness} = \left(\frac{C_{Ca}}{40} + \frac{C_{Mg}}{24}\right) \times 100 \tag{4}$$

where C_{Ca} is the concentration of Ca^{2+} and C_{Mg} is the concentration of Mg^{2+}.

The observed rejection ($R_{i,obs}$) and real rejection ($R_{i,m}$) in the experiments are calculated with the following equations:

$$R_{i,obs} = \left(1 - \frac{C_{i,p}}{C_{i,f}}\right) \times 100\% \tag{5}$$

$$R_{i,m} = \left(1 - \frac{C_{i,p}}{C_{i,m}}\right) \times 100\% \tag{6}$$

where $C_{i,p}$ is the permeate concentration of solute i, $C_{i,f}$ is the feed concentration of solute i and $C_{i,m}$ is the concentration of solute i at feed-and-membrane interface.

According to the film model [27], the relationship between $R_{i,m}$ and $R_{i,obs}$ are given in:

$$\ln\left(\frac{1 - R_{i,obs}}{R_{i,obs}}\right) = \ln\left(\frac{1 - R_{i,m}}{R_{i,m}}\right) + \frac{J_s}{k} \tag{7}$$

$$k = Ku^{0.875} \tag{8}$$

where J_s is the flux speed, k is the mass transfer coefficient, K is the constant and u is the flow velocity (0.116 m/s).

At the meantime, k can also be obtained from Deissler correlation as the following equations [28]:

$$\text{Sh} = 0.065\,\text{Re}^{0.875}\,\text{Sc}^{0.25} \tag{9}$$

$$\text{Sh} = \frac{kd_H}{D},\ \text{Re} = \frac{\eta}{\rho D} \text{ and } \text{Sc} = \frac{u\rho d_H}{\eta} \tag{10}$$

$$D = \frac{(z_+ - z_-)D_+ D_-}{z_+ D_+ - z_- D_-} \tag{11}$$

where hydraulic diameter d_H = 2.475 × 10^{-3} m, dynamic viscosity η = 0.8 × 10^{-3} Pa·s, density of the aqueous solution ρ = 1 × 10^3 kg/m^3, Ca^{2+} diffusion coefficient D_+ = 0.78 × 10^{-9} m^2/s, Cl^- diffusion coefficient D_- = 2.03 × 10^{-9} m^2/s, z_+ the valance of Ca^{2+}, z_- the valance of Cl^- and D diffusion coefficient of $CaCl_2$.

Volumetric membrane charge density (X_d) is calculated with Eq. (12) from zeta-potential (ζ) and membrane pore radius (r_p) through the Gouy–Chapman equation [29]:

$$X_d = \frac{2\text{sign}(\zeta)\sqrt{2\varepsilon_0\varepsilon_b RT\sum_{i=1}^{n} C_{i,f}\left[\exp\left(-\frac{z_i F\zeta}{RT}\right) - 1\right]}}{Fr_p} \tag{12}$$

where ε_0 permittivity, ε_b dielectric constant of the bulk solution, z_i valance of solute i, R gas constant, T absolute temperature and F Faraday constant. Zeta-potential ζ was estimated by tangential streaming potential measurement.

2.3. Taguchi design and analysis of variance

Taguchi design and ANOVA were applied as the experimental arrangement and the statistical evaluation, respectively. TMP, CFV and VRF were investigated as the operative parameters for their effects on the total hardness elimination.

Main steps in Taguchi design include: (1) determining the level (or value) for each parameter, (2) selecting the orthogonal array, (3) conducting experiments based on the array and (4) analyzing the experimental results with signal-to-noise (S/N) ratios. Three parameters of CFV (0.116, 0.136 and 0.207 m/s), TMP (0.8, 1.2 and 1.6 MPa) and instant VRF (increasing from 1 to 4, 1 to 6 and 1 to 8) were selected, correspondingly, L_9 (3^4) orthogonal array was employed to arrange the experiments as listed in Table 1. The S/N ratio has typical three models: the-smaller-the-better, the-larger-the-better and the-nominal-the-best. In our study, the removal ratio of total hardness is expected as large as possible, therefore, the-larger-the-better S/N ratio is chosen consequently. The S/N ratio is related to the performance value (y_i, obtained from the experiment) with Eq. (13):

$$\text{The-larger-the-better S/N} = -10\log_{10}\frac{1}{n}\left(\sum_{i=1}^{n}\frac{1}{y_i^2}\right) \tag{13}$$

The theoretical optimal performance value (y_{opt}) referring to membrane separation performance with the optimized conditions can be predicted with Eq. (14):

$$y_{opt} = \frac{T_t}{n} + \left(A_i - \frac{T_t}{n}\right) + \left(B_i - \frac{T_t}{n}\right) + \ldots \tag{14}$$

where T_t the sum of all observations, n the number of experiments, A_i the average of responses at levels i of factor A and B_i the average of responses at levels i of factor B.

ANOVA is the method to evaluate the impact factors of CFV, TMP and VRF in the membrane process, as well as the correlation between obtained individual data. In this method, sum of squares (SS), degrees of freedom (DOF), mean of square (MS) and associated F test of significance (F_T) are defined as following:

$$\mathrm{SS}_T = \sum_{i=1}^{n} x_i^2 - \frac{1}{n}\left(\sum_{i=1}^{n} y_i\right)^2 \tag{15}$$

$$\mathrm{SS}_j = \frac{1}{r}\sum_{i=1}^{m} K_{ij}^2 - \frac{1}{n}\left(\sum_{1}^{n} y_i\right)^2 \tag{16}$$

where SS_T is the total SS, SS_j is the SS of parameter j, m is the level of parameter j and r is defined as $r = n/m$. The relationship of SS is described as:

$$\mathrm{SS}_T = \mathrm{SS}_1 + \mathrm{SS}_2 + \ldots + \mathrm{SS}_j + \ldots + \mathrm{SS}_e \tag{17}$$

where SS_e is SS of error.

$$\mathrm{DOF}_T = n - 1 \tag{18}$$

$$\mathrm{DOF}_j = m - 1 \tag{19}$$

where DOF_T is the total DOF and DOF_j is the DOF of parameter j.

$$\mathrm{MS} = \frac{\mathrm{SS}}{\mathrm{DOF}} \tag{20}$$

$$F_{T,j} = \frac{\mathrm{MS}_j}{\mathrm{MS}_e} \tag{21}$$

where F_j is the F of parameter j, MS_j is the MS of parameter j and MS_e is the MS of parameter j.

Contribution is defined as follows:

$$\text{Contribution} = \frac{\mathrm{SS}_j}{\mathrm{SS}_T} \times 100\% \tag{22}$$

Table 1
Taguchi-designed L_9 (3^4) orthogonal array for the experiments on NF membrane process with the results on hardness removal and the performance-dependent S/N ratios

Experiment no.	Parameters			Response values: removal ratio of total hardness (%)	S/N ratios (dB)
	CFV (m/s)	TMP (MPa)	VRF		
1	0.116	0.8	1 → 4	77.05	37.73
2	0.116	1.2	1 → 6	80.33	38.10
3	0.116	1.6	1 → 8	79.37	38.03
4	0.136	0.8	1 → 6	63.44	36.05
5	0.136	1.2	1 → 8	68.71	36.74
6	0.136	1.6	1 → 4	73.55	37.33
7	0.207	0.8	1 → 8	66.64	36.47
8	0.207	1.2	1 → 4	72.04	37.15
9	0.207	1.6	1 → 6	74.96	37.50

3. Results and discussion

3.1. NF membrane treating the RO concentrate

NF membrane process used to eliminate the total hardness in wastewater source has been operated by varying parameters CFV, TMP and VRF in nine rounds of experiment following the Taguchi array. Each parameter has a corresponding level (or value) and the optimal level is determined when the maximum S/N ratio is reached. As presented in Table 1, the measured removal ratios of total hardness by the NF membrane change from 63.4% to 80.3% under different operating conditions.

3.1.1. Influence of CFV, TMP and VRF on process efficiency

Wastewater flux (J) passing though the membrane was first studied as varying the three process parameters of CFV, TMP and VRF (Fig. 3). In general, the flux constantly increased when raising the pressure difference TMP and the impact of flow speed CFV on J is depending on the change of TMP. On the other hand, wastewater flux declined as the total solution volume was reduced as a function of test duration. Decreasing J along with instant volume reduction VRF_t changing from 1 to large values (Fig. 3) is properly caused by concentration polarization. The polarization, referring that the species rejected by the membrane develops a layer of higher concentration near the membrane surface than that of the bulk solution, forms an additional layer that can weaken the net effect of flux. At the meantime, contaminants are more easily accumulated on membrane surface at higher concentration (i.e., larger VRF).

Justification on the optimal levels of CFV, TMP and VRF parameters regarding to membrane rejection to hardness ions with analysis of their S/N ratios is presented in Fig. 4. The slowest CFV = 0.116 m/s, highest TMP = 1.6 MPa and smallest VRF = 4 were selected as the optimal conditions as all having the highest S/N ratios. It can be presumed that a "filtration" layer could be formed on membrane surface more spontaneously with slower surface flow leading to more apparent rejection to Ca^{2+} and Mg^{2+} ions. Greater pressure drives the faster flux though the membrane and the solvent permeability (H_2O molecules) exceed the solute permeability (Ca^{2+} and Mg^{2+}) under higher pressure. Then the faster water flux diluted the permeate solution which resulted in a larger retention of the hardness ions [30]. One possible explanation is that the cake-enhanced concentration polarization and the presence of cake layer may prevent the solutes diffusing from the membrane boundary back to the bulk solution [31].

As a summary, the optimized parameters in NF membrane process for the greatest retention of hardness ions were obtained as CFV = 0.116 m/s, TMP = 1.6 MPa and VRF_t = 4 based on the Taguchi-arranged experiments.

3.1.2. Statistical evaluation on the parameters

In parallel, ANOVA provides statistic information on how significant the interested parameters are in the process, whose results are listed in Table 2 based on Eqs. (13)–(22) calculations. In the table, "F-value" is useful to qualify the factorial effect and the "Contribution" percentage gives quantitative accounts about the parameter importance. The evaluation results are only considered reliable when the error contribution is less than 50%, which refers to the background noise caused by uncontrollable parameters. In our study, the contribution of error was 2.4% far less than the critical value providing that the experimental noise was ignorable.

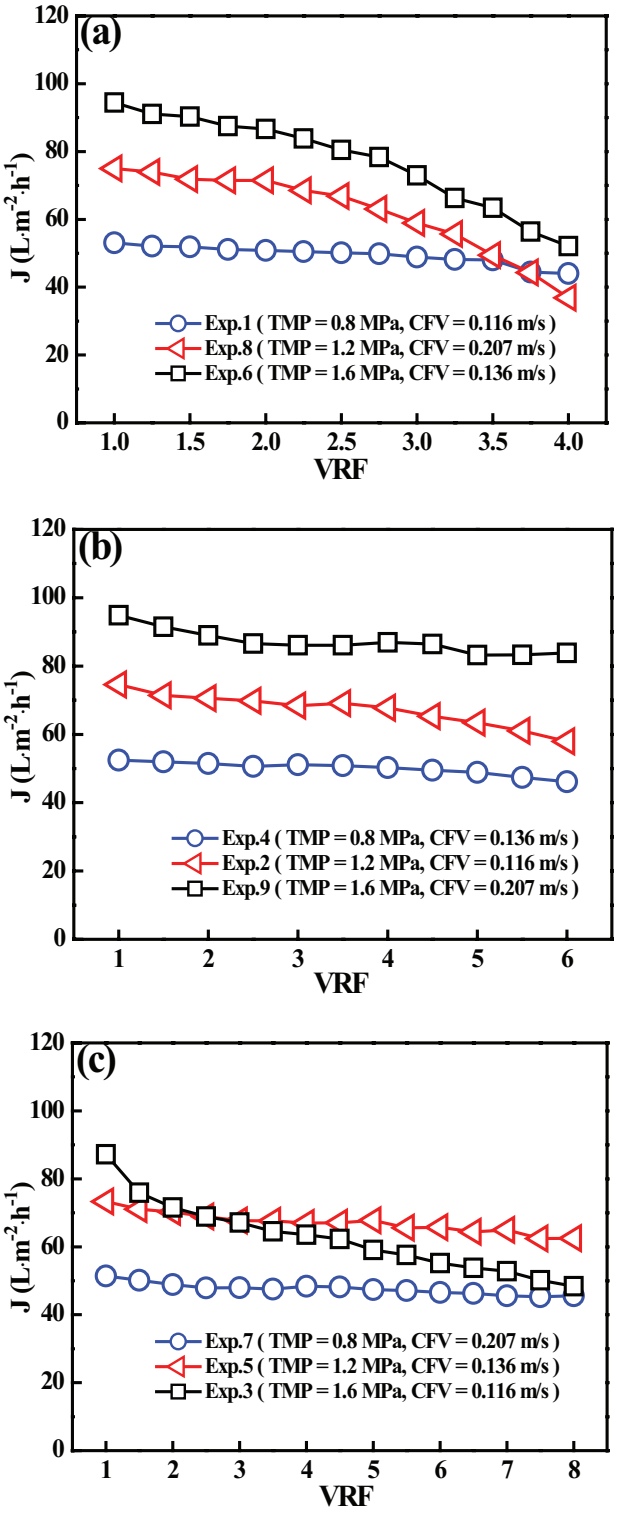

Fig. 3. Effect of process parameters CFV, TMP and VRF on water flux (J) through the NF membrane.

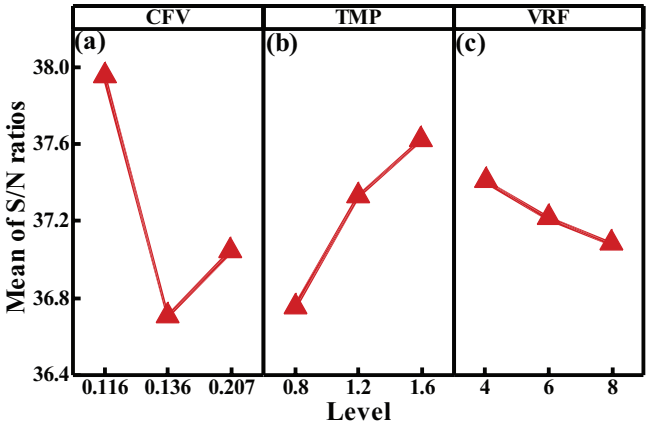

Fig. 4. S/N ratio analysis of each parameter (CFV, TMP and VRF) based on their performance value (i.e., removal of total hardness).

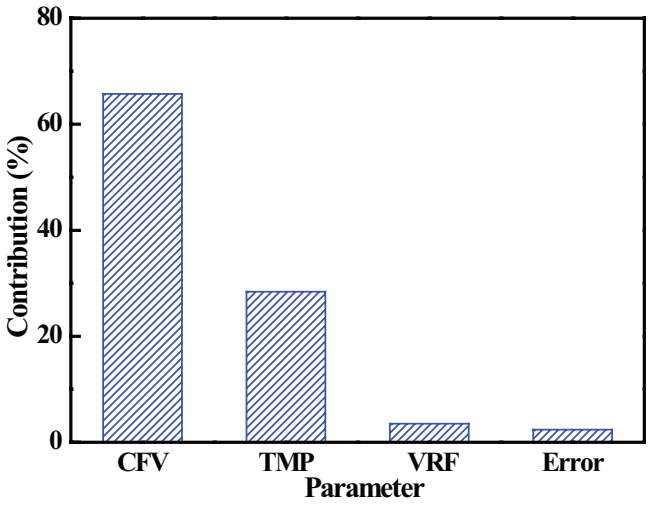

Fig. 5. Contribution of each parameter on the process efficiency based on the analysis of variance (ANOVA).

Table 2
Analysis of variance (ANOVA) on each parameter to evaluate the relevant significance contribution in the NF membrane process

Parameters	DOF	SS	MS	*F* values	Contribution (%)
CFV	2	177.8	88.9	27.3	65.7
TMP	2	76.8	38.4	11.8	28.4
VRF_t	2	9.5	4.8	1.5	3.5
Error	2	6.5	3.3	–	2.4
Total	8	270.6	–	–	100.0

F value is an index to examine the parameter significance on membrane separation to metal ions in water. When the calculated *F* value is bigger than the tabulated value, then the parameter has significant effect at each confidence level. In this work, the tabulated value is 19 at its confidence level 95% [25]. As given in Table 2, the *F* values for CFV, TMP and VRF suggest that CFV (velocity) having *F* value over 19 should perform significant impact in the NF process.

As displayed in Fig. 5, "Contribution" impact of CFV, TMP and VRF consistently indicates that the hydrodynamic conditions including CFV and TMP have stronger correlation with membrane separation performance in comparison with VRF. In a summary, the importance of operation parameter ranks as CFV > TMP > VRF.

3.1.3. NF membrane process operated with the optimal parameters

3.1.3.1. Confirmative test to Taguchi-designed experiments After the parameters have been found, confirmative experiments were carried out under the selected conditions to complete the optimization work. The results of the additional tests, using the same experimental setup as the previous nine tests, are recorded in Table 3: total hardness (433 mg/L), sulfate (24 mg/L), TDS (1,157 mg/L), COD (13 mg/L) and turbidity (0.2 NTU). All the contents in the NF permeate are lower than the critical values in water reuse standard, whereas, the RO concentrate could not satisfy these standards. Removal of the total hardness was up to 84%, sulfate 96%, COD 96% and TDS 63% in the NF membrane process. On the other hand, the experimental result on hardness reduction from the confirmative test is 84% which has no apparent difference to the theoretical value as 83% which is calculated according to Eq. (13) under the optimal conditions. Hence, it ensures that the optimized parameters CFV = 0.116 m/s, TMP = 1.6 MPa and VRF_t = 4 can be determined in NF membrane process as treating RO concentrate of paper mill effluents.

3.1.3.2. Long-term test with the continuous feed supply Based on the previous work, a long-term NF process test operated with CFV 0.116 m/s and TMP 1.6 MPa was carried out at the paper mill location for 114 h using continuous feed supply of concentrated wastewater from RO process. Recorded wastewater flux and removal of total hardness in the NF membrane process are plotted along with filtration hours, respectively. Wastewater flux (*J*) reduced apparently from 90 to 27 L/m²/h in the first 20 h properly due to fouling deposition on the surface (Fig. 6). Further on, a gradual decline of *J* was observed as the fouling rate could be decreasing and then *J* maintained at 15 L/m²/h during the whole following filtration till over 100 h. Meanwhile, the removal ratio of hardness ions decreased from 83% to 80% in the first 20 h and later on became relatively stable at 76% lasting to 114 h (Fig. 7). The cake-enhanced osmotic pressure from permeate side to feed side could be enforced with the appearance of concentration polarization [31]. Such osmotic pressure could contribute the "dilute effect" of the solution in feed side and result in the reduced retention.

3.2. Effect of salt concentration on NF membrane rejection

We have found that the membrane rejection to the hardness divalent ions in water climbed up by increasing solution concentration in all the Taguchi experiments as presented in Fig. 8. Similar results have been reported that higher solute rejection was obtained at higher feed concentration in the case of using polymeric membrane to separate divalent cations [32,33]. However, concrete explanation thereby was not

Table 3
Experimental results on the quality of feed, retentate and permeate in the membrane process under the optimized conditions

Items	Feed (RO concentrate)	Retentate (NF)	Permeate (NF)	Rejection (%)	Reuse standard
Total hardness, mg/L	1,047 ± 25	2,727 ± 42	433 ± 12	84 ± 0.2	≤450[a]
Ca^{2+}, mg/L	395 ± 13	999 ± 22	165 ± 7	83 ± 0.3	N.A.
Mg^{2+}, mg/L	14 ± 2	55 ± 3	5 ± 1	92 ± 1.4	N.A.
Sulfate, mg/L	198 ± 4	686 ± 14	24 ± 1	96 ± 0.2	≤250[a]
TDS, mg/L	1,907 ± 12	3,087 ± 12	1,157 ± 6	63 ± 0.3	≤1,500[a]
COD, mg/L	113 ± 6	293 ± 6	13 ± 1	96 ± 0.4	≤60[a]
pH	7.9 ± 0.1	8.0 ± 0.1	7.9 ± 0.1	–	6.5–9.0[a]
Turbidity, NTU	0.4 ± 0.2	0.7 ± 0.2	0.2 ± 0.1	–	<1.0[b]
SDI	1.2 ± 0.1	2.6 ± 0.2	0.8 ± 0.1	–	<5.0[b]

N.A., not available.
[a]According to the reuse of urban recycling water (GB/T 18919-2002, China).
[b]According to the reverse osmosis water treatment equipment (GB/T 19249-2003, China).

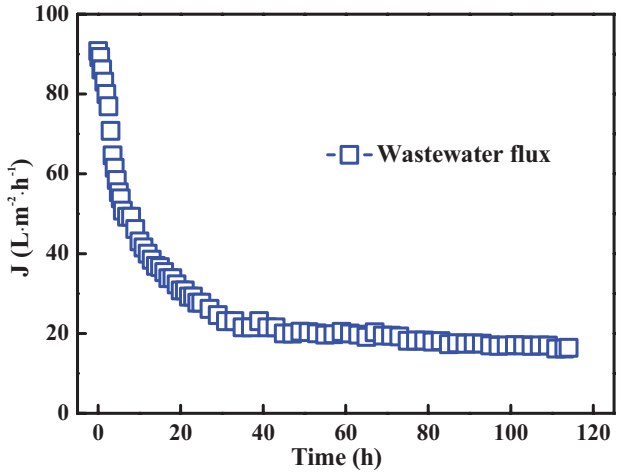

Fig. 6. Water flux (J) through the NF membrane in the long-term test.

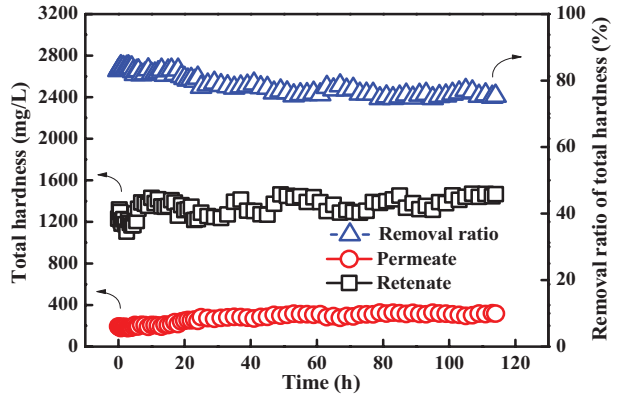

Fig. 7. Removal ratio of total hardness (Δ), ions concentrate in retentate (□) and ions concentration in permeate (○) in the long-term test.

given. In this session, we investigated various concentration of $CaCl_2/H_2O$ as feed solution to understand the relationship between ions retention vs. solute concentration. We shall discuss the real rejection (R_i) and the membrane charge density (X_d) in details in order to clarify the concentration-dependent membrane behavior.

3.2.1. Mass transfer coefficient measurement for real rejection ($R_{i,m}$)

When the concentration polarization cannot be neglected in the membrane process, the real rejection of solute i ($R_{i,m}$) is related to the observed rejection ($R_{i,obs}$) through the mass transfer coefficient (k) that can be obtained with the velocity variation method [34]. According to Eqs. (7) and (8), k is proportional to factor K and $1/K$ is indicated as the slope of curves by plotting $\ln[(1 - R_{i,obs})/R_{i,obs}]$ as a function of $J_s/u^{0.875}$ as presented in Fig. 9. As a result, k is found in the range of 2.40×10^{-5} and 3.46×10^{-5} m/s.

The theoretical value of k has also been obtained as 2.82×10^{-5} m/s from Deissler correlation according to Eqs. (9)–(11). As a result, the mass transfer coefficients obtained experimentally ($k = 2.40 - 3.46 \times 10^{-5}$ m/s) and theoretically ($k = 2.82 \times 10^{-5}$ m/s) are in a good agreement. Therefore, k value from Deissler correlation is reasonable to estimate the concentration polarization effect and subsequently the $R_{i,m}$ value is calculated with Eqs. (7) and (8).

3.2.2. Explanation with charge density (X_d) for the concentration effect

Rejection to Ca^{2+} was gradually enhanced as increasing feed concentration of $CaCl_2$ from 1, 5 to 10 mol/m^3 at the same TMP (Fig. 11). As for the membrane process dealing with charged species: diffusion, electromigration and convection are accounted to understand the mass transfer and relevant numerical calculations are described in many works [35–37]. In low concentration (like in our work), migration to electrostatic interaction, convection to pressure difference and steric exclusion in nanochannels are the major factors affecting permeability and selectivity of the membrane.

First of all, interaction between the $CaCl_2$ solute and polymeric membrane was studied with volumetric membrane charge density (X_d). The value of X_d is to be determined based on Eq. (12) when knowing mean pore radius (r_p) and zeta-potential (ζ). The r_p value was acquired from the filtration

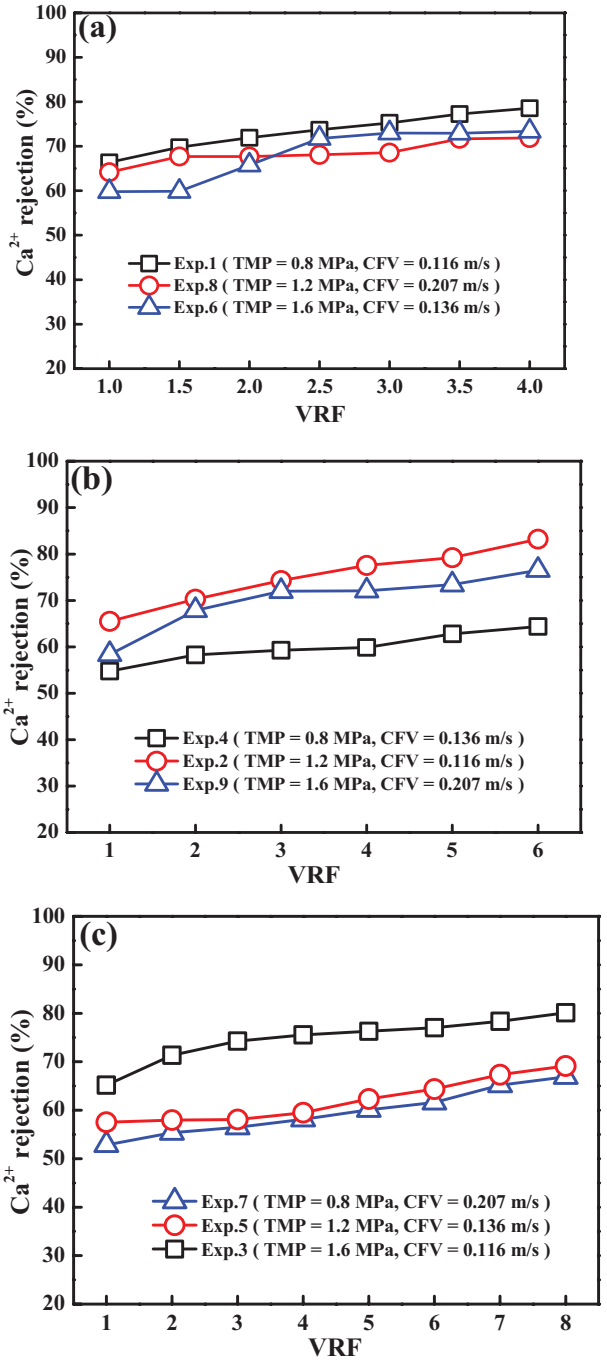

Fig. 8. Effect of membrane process parameters CFV, TMP and VRF on Ca^{2+} rejection.

tests using uncharged solute (glucose) in water by plotting glucose rejection to flux speed (J_s) at two different concentrations (Fig. 10). The rejection curve raised to a plateau with increasing J_s and the data were fitted with Spiegler–Kedem and steric hindrance pore model to calculate r_p, whose hypothesis and calculation procedures are detailed elsewhere [36]. As a result, effective pore radius was found as 0.391 nm using glucose solution 300 mg/L and 0.384 nm using 500 mg/L. The averaged value of r_p is known to be 0.388 nm for the NF membrane. DL membrane was negatively charged and

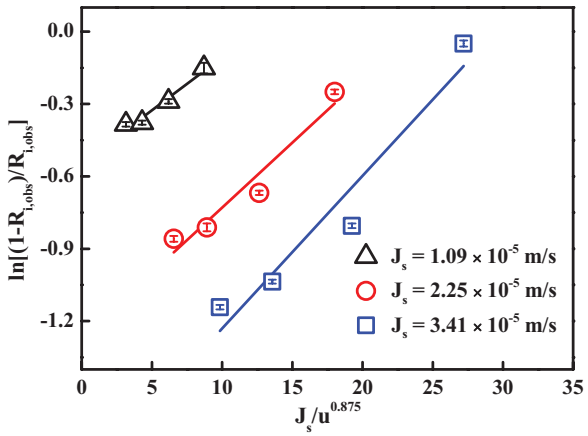

Fig. 9. Determination of mass transfer coefficient k (as the curve slopes) in the situation using model solution $CaCl_2/H_2O$ 10 mol/m^3.

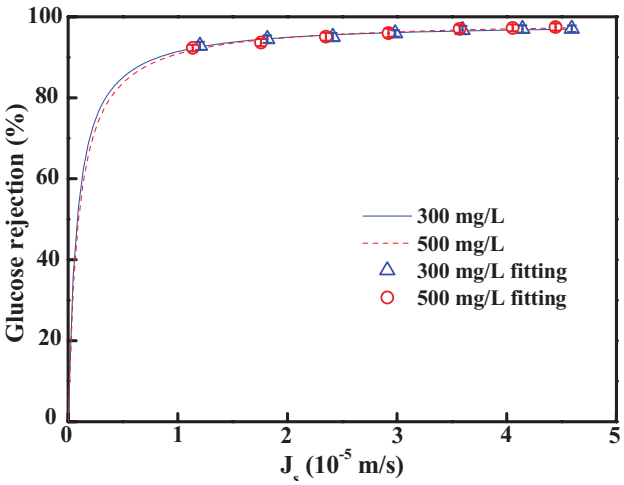

Fig. 10. Determination of mean pore size (r_p) by fitting the membrane's rejection to glucose as a function of flux speed.

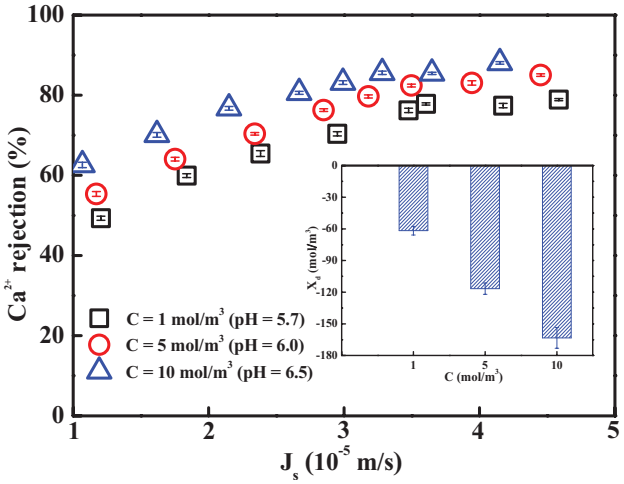

Fig. 11. Membrane rejection to Ca^{2+} and volume membrane charge density (X_d) at different concentrations of $CaCl_2/H_2O$ model solution.

its zeta-potential (ζ) was measured as immersing in $CaCl_2$/H_2O solution. Correspondingly, the charge density of membrane (X_d) was intensified from –62, –117 to –163 mol/m^3 with increased $CaCl_2$ concentration from 1, 5 to 10 mol/m^3 as presented in Fig. 11.

Other researchers have reported analogous results that polyamide NF membrane was negatively charged and X_d absolute value grew with concentration and pH [38–40]. Progressive adsorption of anions (Cl^-) prevailed the governing mechanisms of membrane's negative charge formation [39–42]. Hydrated radius of Cl^- is smaller than that of Ca^{2+} [43,44] and Cl^- is also less and weakly hydrated [43–46] so that the monovalent anions are preferentially approaching and staying on the membrane surface with less steric hindrance. Good fitting between the charge density growth and adsorption isotherms is coherent to this mechanism [47–50]. Such high X_d could be formed due to nanoporous medium's large surface-to-volume ratio and it excluded electrical neutrality on the membrane surface in the studied salt concentrations [50]. Isoelectric point of the membrane DL membrane (from GE) was reported to be pH 3.0 [40] and it is reasonable to observe larger X_d absolute value at higher initial pH from 5.7 to 6.5 that has a greater alteration from its isoelectric point [39].

Some other studies have revealed that a potential difference existed on the membrane surface and in the pores: potential reduced from the surface to the passing nanochannels [49]. It precludes stronger electrostatic attraction to divalent cations crossing the membrane, given that Ca^{2+} ions are allowed transferring from the bulk solution to the membrane surface [43]. Meanwhile, effect pore dimensions are narrowed when negatively charged groups in the pores adopt an extended conformation due to electrostatic repulsion [51–53]. Both potential difference and steric exclusion could prevent Ca^{2+} ions (hydrated radius 0.412 nm) to penetrate the NF membrane (mean pore radius 0.388 nm). The accumulated cations in the near of membrane, not permeating the membrane, play as resistance species being repulsive to following Ca^{2+} in flow. It helps to understand that the membrane presents declining flux (at the same TMP) and increasing selectivity to Ca^{2+} when salt concentration went up from 1 to 10 mol/m^3 (Fig. 11).

On the other hand, higher rejection Ca^{2+} ions was witnessed at faster flux speed (J_s) using feed solution of the same concentration as displayed in Fig. 11, which can be explained by the difference in permeability between solute and solvent changing at various J_s. With slower flux, diffusion is the main driving force and the permeate solution would be rich in solute leading to less ions retention. With faster flux, convection flow plays an important role in mass transfer and more divalent cations could be maintained in the retentate side as the water molecules accelerated to pass through the membrane.

4. Conclusions

This work has proposed an effective approach to combine RO treatment with NF membrane process to clean industrial wastewater and recycle the water sources. Commercial polyamide DL NF membrane has been proved suitable to separate hardness ions Ca^{2+} and Mg^{2+} and contaminants of sulfate and CODs from the RO concentrate of paper mill wastewater. Experimental results indicated that the optimal conditions in NF membrane process are with relatively low CFV 0.116 m/s, relatively high TMP 1.6 MPa and VRF_t to 4. Hydrodynamic factors CFV and TMP had strong significance on process efficiency with contribution up to 65.7% and 28.4%, respectively. Under the optimized conditions 84% total hardness, 96% sulfate and 96% CODs were removed and 75% reuse-standard water was recovered after NF process treatment. In the 114 h long-term test, the membrane achieved stable separation performance with the total hardness reduction by 76%. It is interesting to find out that the rejection to Ca^{2+} ions went up as increasing concentration of $CaCl_2$/H_2O concentration from 1 to 10 mol/m^3. The polyamide membrane was negatively charged in $CaCl_2$ solution with progressive adsorption Cl^- mechanism and X_d (absolute values) grew with higher salt concentration and pH. The Ca^{2+} ions that approached but not penetrated the membrane due to steric and potential aspects could form resistance layer repulsive to coming-up Ca^{2+} in flow. At higher salt concentration, the effect was more prevailing which led to higher Ca^{2+} rejection but at a cost of lower water flux. In a conclusion, the optimized NF membrane process has been confirmed as a reliable means to treat industrial wastewater and reduce its hardness after dual UF/RO process without using or producing any chemicals in the system.

Acknowledgments

Sincere thanks to the financial support from the Prospective Joint Research Project of Jiangsu Province (BY2014005-06), the Innovative Research Team Program by the Ministry of Education of China (No. IRT13070), the project funded by the Priority Academic Program Development of Jiangsu Higher Education Institutions (PAPD) of China and the Jiangsu National Synergetic Innovation Center for Advanced Materials (SICAM).

References

[1] M. Vepsalainen, H. Kivisaari, M. Pulliainen, A. Oikari, M. Sillanpaa, Removal of toxic pollutants from pulp mill effluents by electrocoagulation, Sep. Purif. Technol., 81 (2011) 141–150.
[2] O. Ashrafi, L. Yerushalmi, F. Haghighat, Application of dynamic models to estimate greenhouse gas emission by wastewater treatment plants of the pulp and paper industry, Environ. Sci. Pollut. Res., 20 (2013) 1858–1869.
[3] A. Pizzichini, C. Russo, C.D. Meo, Purification of pulp and paper wastewater, with membrane technology, for water reuse in a closed loop, Desalination, 178 (2005) 351–359.
[4] M. Manttari, M. Kuosa, J. Kallas, M. Nystrom, Membrane filtration and ozone treatment of biologically treated effluents from the pulp and paper industry, J. Membr. Sci., 309 (2008) 112–119.
[5] A.Y. Bagastyo, J. Keller, Y. Poussade, D.J. Batstone, Characterisation and removal of recalcitrants in reverse osmosis concentrates from water reclamation plants, Water Res., 45 (2011) 2415–2427.
[6] A.P. Gonzalez, R. Ibanez, P. Gomez, A.M. Urtiaga, I. Ortiz, J.A. Irabien, Nanofiltration separation of polyvalent and monovalent anions in desalination brines, J. Membr. Sci., 473 (2015) 16–27.
[7] P. Westerhoff, H. Moon, D. Minakata, J. Crittenden, Oxidation of organics in retentates from reverse osmosis wastewater reuse facilities, Water Res., 43 (2009) 3992–3998.
[8] T. Zhou, T.T. Lim, S.S. Chin, A.G. Fane, Treatment of organics in reverse osmosis concentrate from a municipal wastewater reclamation plant: feasibility test of advanced oxidation processes with/without pretreatment, Chem. Eng. J., 166 (2011) 932–939.

[9] E. Dialynas, D. Mantzavinos, E. Diamadopoulos, Advanced treatment of the reverse osmosis concentrate produced during reclamation of municipal wastewater, Water Res., 42 (2008) 4603–4608.
[10] B.V. Bruggen, A. Koninckx, C. Vandecasteele, Separation of monovalent and divalent ions from aqueous solution by electrodialysis and nanofiltration, Water Res., 38 (2004) 1347–1353.
[11] F. Zhao, K. Xu, H. Ren, L. Ding, J. Geng, Y. Zhang, Combined effects of organic matter and calcium on biofouling of nanofiltration membranes, J. Membr. Sci., 486 (2015) 177–188.
[12] A.A. Amoudi, R.W. Lovitt, Fouling strategies and the cleaning system of NF membranes and factors affecting cleaning efficiency, J. Membr. Sci., 303 (2007) 6–28.
[13] M. Reig, S. Casas, O. Gibert, C. Valderrama, J.L. Cortina, Integration of nanofiltration and bipolar electrodialysis for valorization of seawater desalination brines: production of drinking and waste water treatment chemicals, Desalination, 382 (2016) 13–20.
[14] N.F. Bishop, O. Nir, O. Lahav, V. Freger, Predicting the rejection of major seawater ions by spiral-wound nanofiltration membranes, Environ. Sci. Technol., 49 (2015) 8631–8638.
[15] T.Y. Liu, C.K. Li, B. Pang, B. Van der Bruggen, X.L. Wang, Fabrication of a dual-layer (CA/PVDF) hollow fiber membrane for RO concentrate treatment, Desalination, 365 (2015) 57–69.
[16] C.M. Tonko, A. Kiraly, P. Mizsey, G. Patzay, E. Csefalvay, Limitation of hardness from thermal water by means of nanofiltration, Water Sci. Technol., 67 (2013) 2025–2032.
[17] G.M. Ayoub, R.M. Zayyat, M.A. Hindi, Precipitation softening: a pretreatment process for seawater desalination, Environ. Sci. Pollut. Res., 21 (2014) 2876–2887.
[18] J. Kaewsuk, D.Y. Lee, T.S. Lee, G.T. Seo, Effect of ion composition on nanofiltration rejection for desalination pretreatment, Desal. Wat. Treat., 43 (2012) 260–266.
[19] H. Saitua, R. Gil, A.P. Padilla, Experimental investigation on arsenic removal with a nanofiltration pilot plant from naturally contaminated groundwater, Desalination, 274 (2011) 1–6.
[20] P. Dydo, M. Turek, J. Ciba, Scaling analysis of nanofiltration systems fed with saturated calcium sulfate solutions in the presence of carbonate ions, Desalination, 159 (2003) 245–251.
[21] A. Zirehpour, A. Rahimpour, M. Jahanshahi, M. Peyravi, Mixed matrix membrane application for olive oil wastewater treatment: process optimization based on Taguchi design method, J. Environ. Manage., 132 (2014) 113–120.
[22] S. Pourjafar, M. Jahanshahi, A. Rahimpour, Optimization of TiO_2 modified poly(vinyl alcohol) thin film composite nanofiltration membranes using Taguchi method, Desalination, 315 (2013) 107–114.
[23] A. Salahi, T. Mohammadi, Oily wastewater treatment by ultrafiltration using Taguchi experimental design, Water Sci. Technol., 63 (2011) 1476–1484.
[24] A. Idris, A.F. Ismail, M.Y. Noordin, S.J. Shilton, Optimization of cellulose acetate hollow fiber reverse osmosis membrane production using Taguchi method, J. Membr. Sci., 205 (2002) 223–237.
[25] Z.W. Song, L.Y. Jiang, Optimization of morphology and performance of PVDF hollow fiber for direct contact membrane distillation using experimental design, Chem. Eng. Sci., 101 (2013) 130–143.
[26] R. Hepsen, Y. Kaya, Optimization of membrane fouling using experimental design: an example from dairy wastewater treatment, Ind. Eng. Chem. Res., 51 (2012) 16074–16084.
[27] J. Fang, B. Deng, Rejection and modeling of arsenate by nanofiltration: contributions of convection, diffusion and electromigration to arsenic transport, J. Membr. Sci., 453 (2014) 42–51.
[28] G. Yang, W. Xing, N. Xu, Concentration polarization in spiral-wound nanofiltration membrane elements, Desalination, 154 (2003) 89–99.
[29] A.I.C. Morao, A. Szymczyk, P. Fievet, A.M.B. Alves, Modelling the separation by nanofiltration of a multi-ionic solution relevant to an industrial process, J. Membr. Sci., 322 (2008) 320–330.
[30] C.V. Gherasim, P. Mikulasek, Influence of operating variables on the removal of heavy metal ions from aqueous solutions by nanofiltration, Desalination, 343 (2014) 67–74.
[31] E.M.V. Hoek, M. Elimelech, Cake-enhanced concentration polarization: a new fouling mechanism for salt-rejecting membranes, Environ. Sci. Technol., 37 (2003) 5581–5588.
[32] G. Hagmeyer, R. Gimbel, Modelling the salt rejection of nanofiltration membranes for ternary ion mixtures and for single salts at different pH values, Desalination, 117 (1998) 247–256.
[33] S. Bandini, D. Vezzani, Nanofiltration modeling: the role of dielectric exclusion in membrane characterization, Chem. Eng. Sci., 58 (2003) 3303–3326.
[34] A.I.C. Morao, A.M.B. Alves, V. Geraldes, Concentration polarization in a reverse osmosis/nanofiltration plate-and-frame membrane module, J. Membr. Sci., 325 (2008) 580–591.
[35] J. Schaep, C. Vandecasteele, A.W. Mohammad, W.R. Bowen, Modelling the retention of ionic components for different nanofiltration membranes, Sep. Purif. Technol., 22–23 (2001) 169–179.
[36] W.R. Bowen, B. Cassey, P. Jones, D.L. Oatley, Modelling the performance of membrane nanofiltration—application to an industrially relevant separation, J. Membr. Sci., 242 (2004) 211–220.
[37] A. Szymczyk, C. Labbez, P. Fievet, A. Vidonne, A. Foissy, J. Pagetti, Contribution of convection, diffusion and migration to electrolyte transport through nanofiltration membranes, Adv. Colloid Interface Sci., 103 (2003) 77–94.
[38] C. Mazzoni, L. Bruni, S. Bandini, Nanofiltration: role of the electrolyte and pH on desal DK performances, Ind. Eng. Chem. Res., 46 (2007) 2254–2262.
[39] M.D. Afonso, Surface charge on loose nanofiltration membranes, Desalination, 191 (2006) 262–272.
[40] A.I.C. Morao, A.M.B. Alves, M.D. Afonso, Concentration of clavulanic acid broths: influence of the membrane surface charge density on NF operation, J. Membr. Sci., 281 (2006) 417–428.
[41] S. Bandini, Modelling the mechanism of charge formation in NF membranes: theory and application, J. Membr. Sci., 264 (2005) 75–86.
[42] C. Labbez, P. Fievet, A. Szymczyk, A. Vidonne, A. Foissy, J. Pagetti, Retention of mineral salts by a polyamide nanofiltration membrane, Sep. Purif. Technol., 30 (2003) 47–55.
[43] B. Tansel, J. Sager, T. Rector, J. Garland, R.F. Strayer, L. Levine, M. Roberts, M. Hummerick, J. Bauer, Significance of hydrated radius and hydration shells on ionic permeability during nanofiltration in dead end and cross flow modes, Sep. Purif. Technol., 51 (2006) 40–47.
[44] A.G. Volkov, S. Paula, D.W. Deamer, Two mechanisms of permeation of small neutral molecules and hydrated ions across phospholipid bilayers, Bioelectrochem. Bioenerg., 42 (1997) 153–160.
[45] J. Zhou, X.H. Lu, Y.R. Wang, J. Shi, Molecular dynamics study on ionic hydration, Fluid Phase Equilib., 194 (2002) 257–270.
[46] H. Binder, O. Zschornig, The effect of metal cations on the phase behavior and hydration characteristics of phospholipid membranes, Chem. Phys. Lipids, 115 (2002) 39–61.
[47] A.E. Childress, M. Elimelech, Effect of solution chemistry on the surface charge of polymeric reverse osmosis and nanofiltration membranes, J. Membr. Sci., 119 (1996) 253–268.
[48] L. Bruni, S. Bandini, The role of the electrolyte on the mechanism of charge formation in polyamide nanofiltration membranes, J. Membr. Sci., 308 (2008) 136–151.
[49] L. Bruni, S. Bandini, Studies on the role of site-binding and competitive adsorption in determining the charge of nanofiltration membranes, Desalination, 241 (2009) 315–330.
[50] S. Deon, A. Escoda, P. Fievet, A transport model considering charge adsorption inside pores to describe salts rejection by nanofiltration membranes, Chem. Eng. Sci., 66 (2011) 2823–2832.
[51] M.R. Teixeira, M.J. Rosa, M. Nystrom, The role of membrane charge on nanofiltration performance, J. Membr. Sci., 265 (2005) 160–166.
[52] A.E. Childress, M. Elimelech, Relating nanofiltration membrane performance to membrane charge (electrokinetic) characteristics, Environ. Sci. Technol., 34 (2000) 3710–3716.
[53] J. Schaep, C. Vandecasteele, Evaluating the charge of nanofiltration membranes, J. Membr. Sci., 188 (2001) 129–136.